Supplement of

Elucidating the pollution characteristics of nitrate, sulfate and ammonium in $PM_{2.5}$ in Chengdu, southwest China based on long-term observations

Liuwei Kong[1], Miao Feng[2], Yafei Liu[1], Yingying Zhang[1], Chen Zhang[1], Chenlu Li[1], Yu Qu[3], Junling An[3], Xingang Liu[1,*], Qinwen Tan[2,*], Nianliang Cheng[4], Yijun Deng[5], Ruixiao Zhai[5], Zheng Wang[5]

[1]State Key Laboratory of Water Environment Simulation, School of Environment, Beijing Normal University, Beijing 100875, China

[2]Chengdu Academy of Environmental Sciences, Chengdu 610072, China

[3]State Key Laboratory of Atmospheric Boundary Layer Physics and Atmospheric Chemistry, Institute of Atmospheric Physics, Chinese Academy of Sciences, Beijing 100029, China

[4]Beijing Municipal Environmental Monitoring Center, Beijing 100048, China

[5]Yuncheng Municipal Ecological Environment Bureau, Yuncheng, 044000, China

* Corresponding author.

E-mail addresses: liuxingang@bnu.edu.cn (Xingang Liu) and 11923345@qq.com (Qinwen Tan)

Table S1. Comparison of $PM_{2.5}$, NO_2 and SO_2 ($\mu g/m^3$)mass concentrations from 2013 to 2017.

	2013	2014	2015	2016	2017
$PM_{2.5}$	97	77	64	63	56
NO_2	63	59	53	54	53
SO_2	31	19	14	14	11

Data from Chengdu Municipal Ecology and Environment Bureau: Ambient air quality report, last access: 12 February 2020

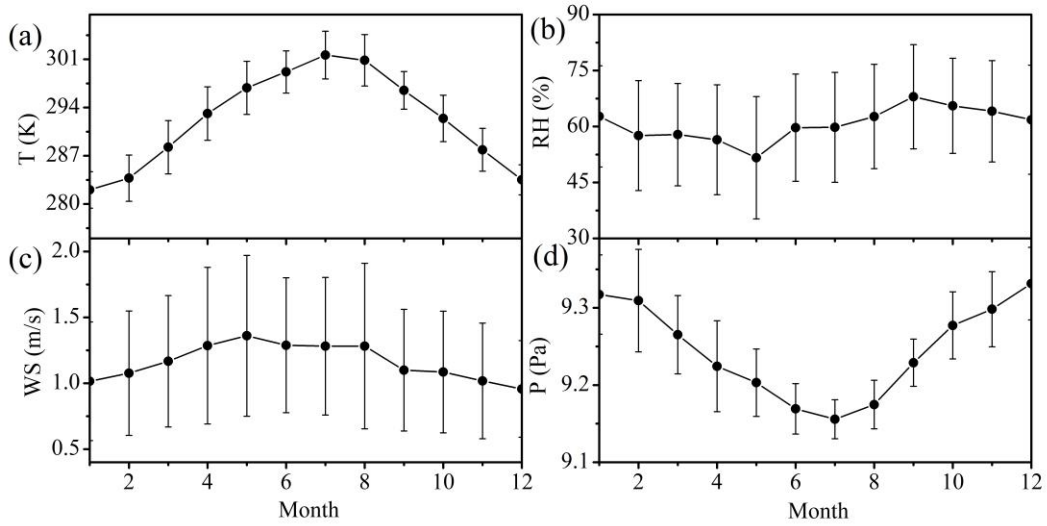

Fig. S1. Monthly variations in meteorological conditions during the observations (2015-2017).

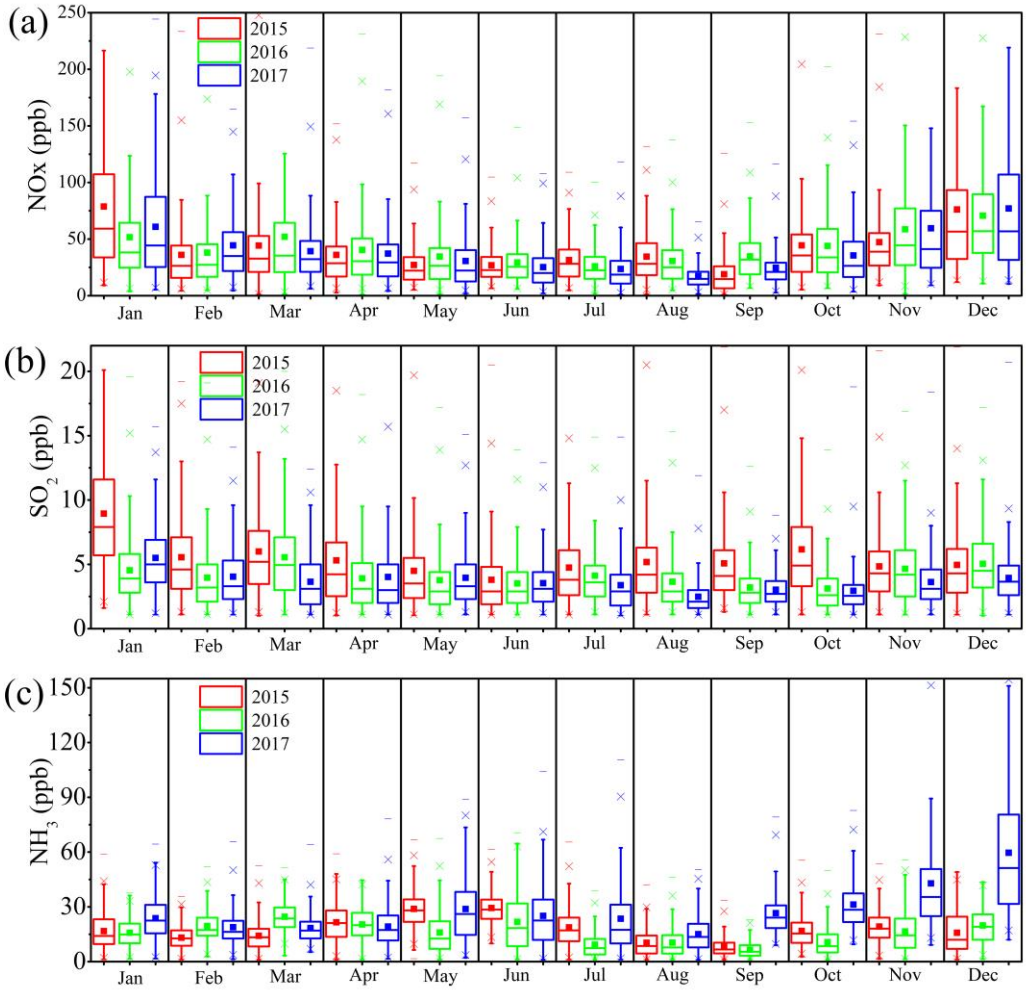

Fig. S2. Monthly variations in NO_2, SO_2 and NH_3 concentrations from 2015 to 2017.

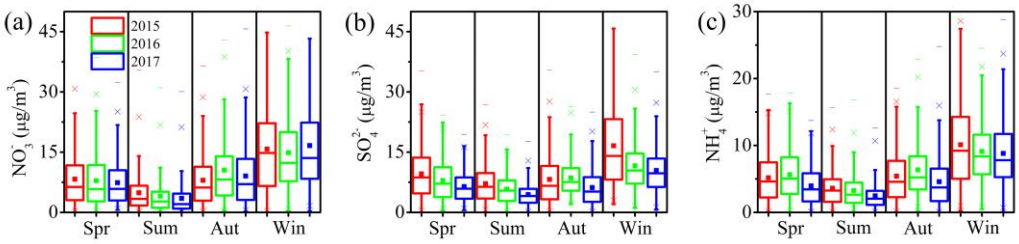

Fig. S3. Seasonal variations in NO_3^-, SO_4^{2-} and NH_4^+ mass concentrations from 2015 to 2017.

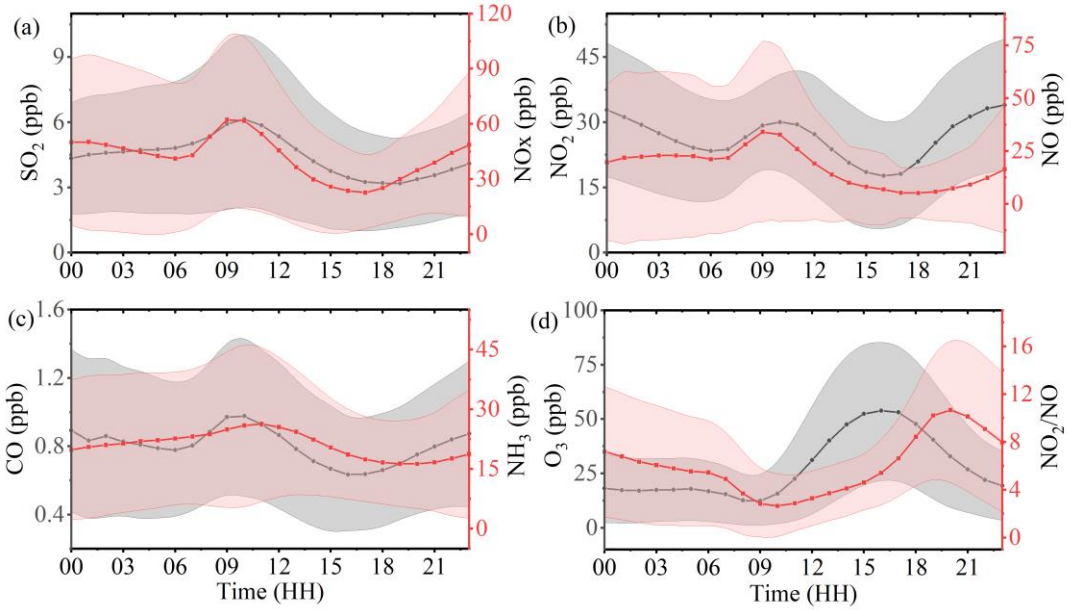

Fig. S4. Diurnal variations in gaseous pollutants from 2015 to 2017.

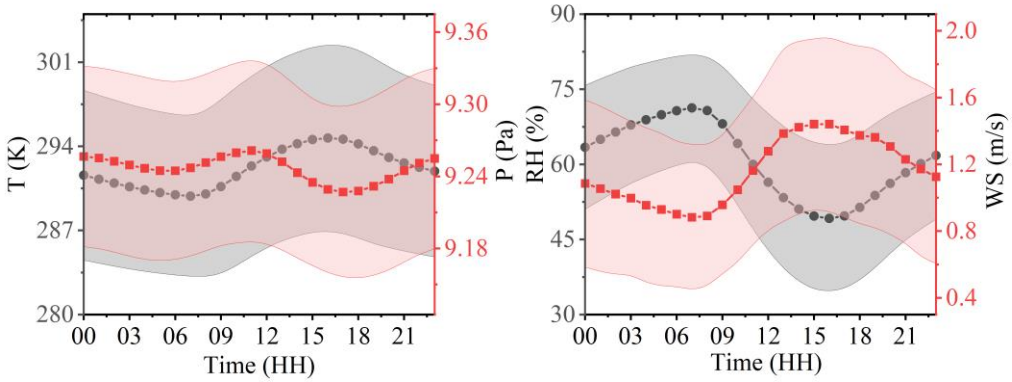

Fig. S5. Diurnal variations in metrological conditions from 2015 to 2017.

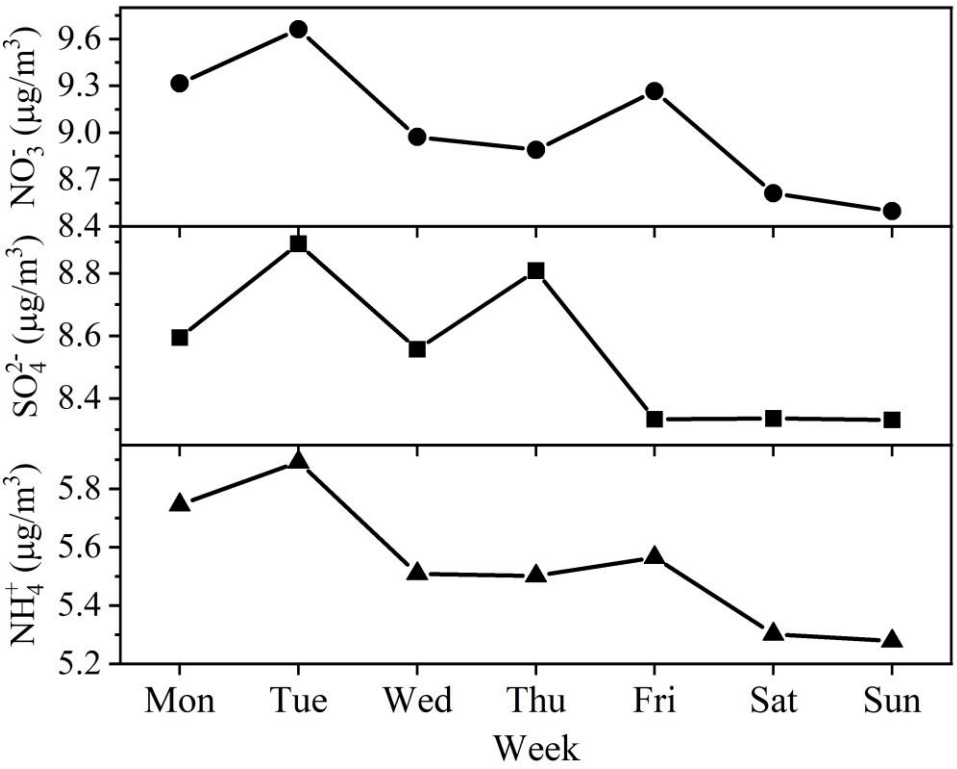

Fig. S6. Weekly variations in NSA during the overall observation period.

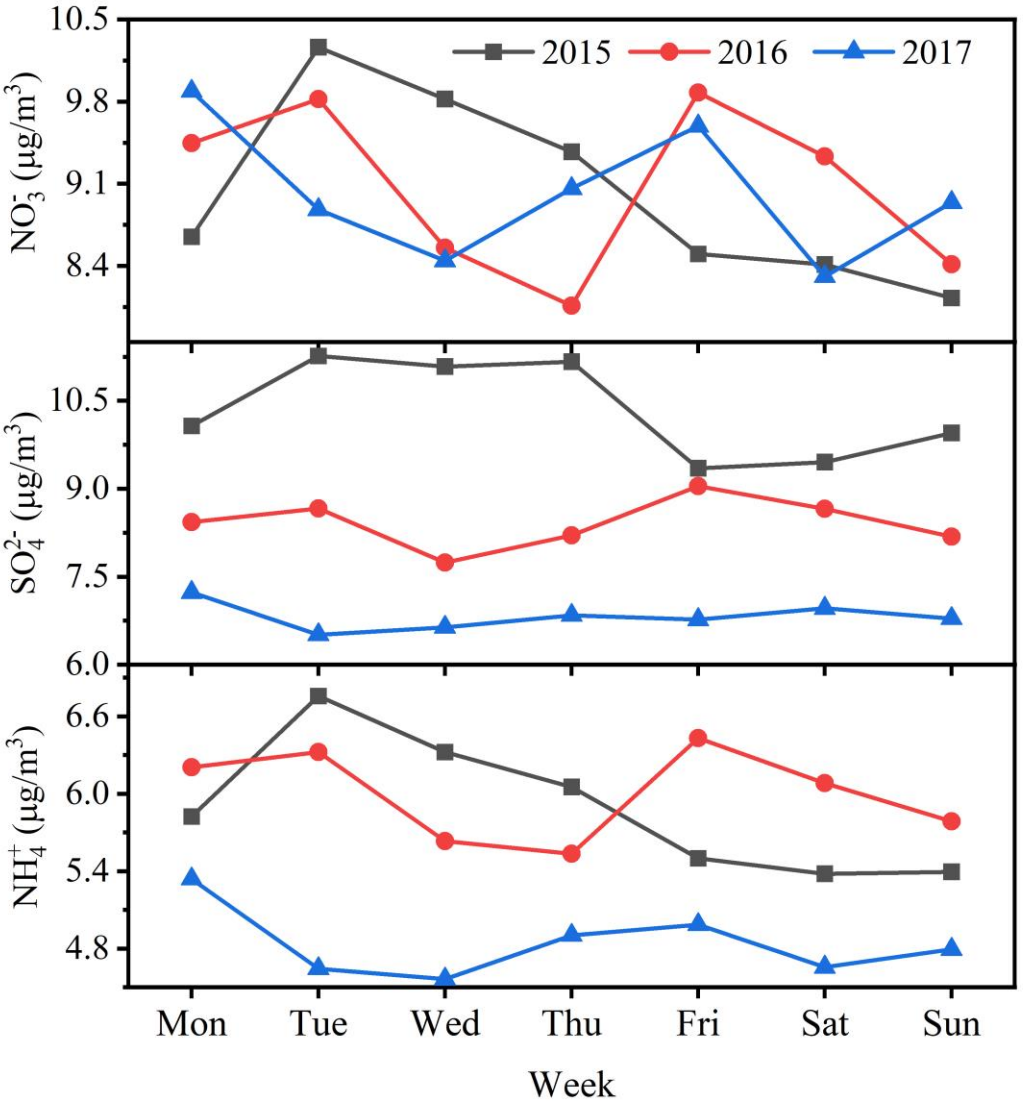

Fig. S7. Weekly variations in NSA from 2015 to 2017 (Broken line diagram).

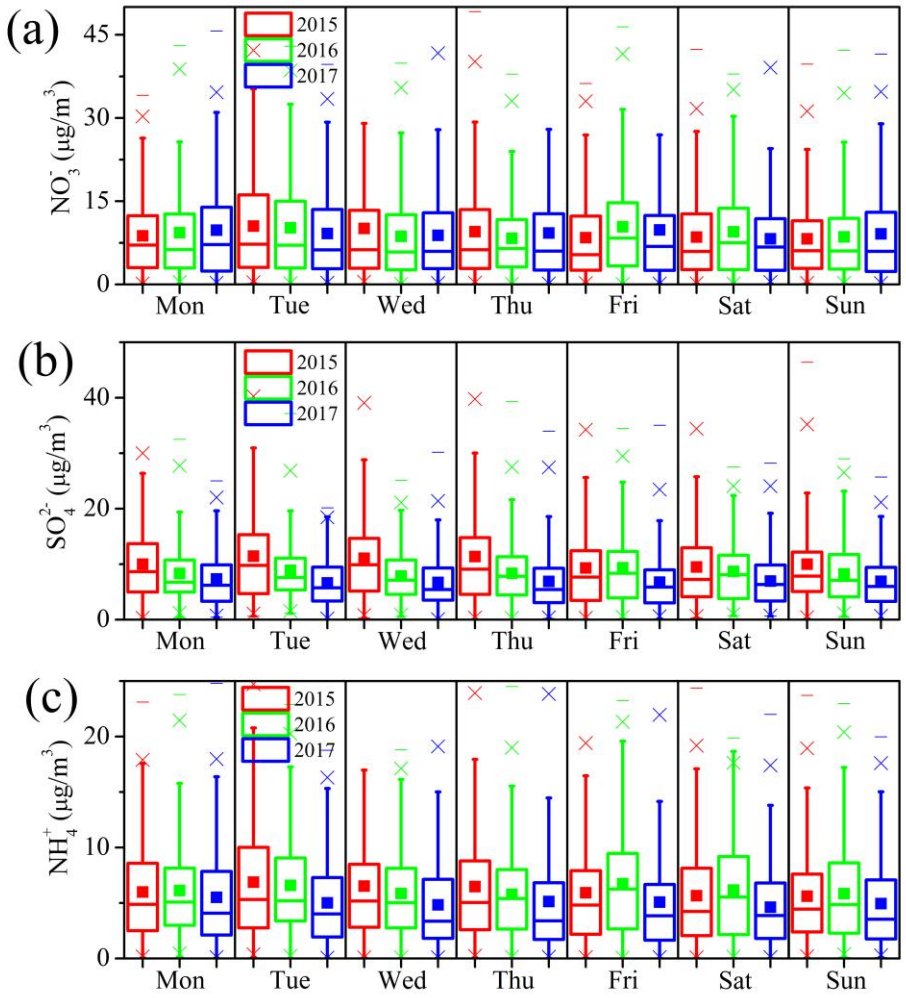

45

46 Fig. S8. Weekly variations in NSA from 2015 to 2017 (Box diagram).

47

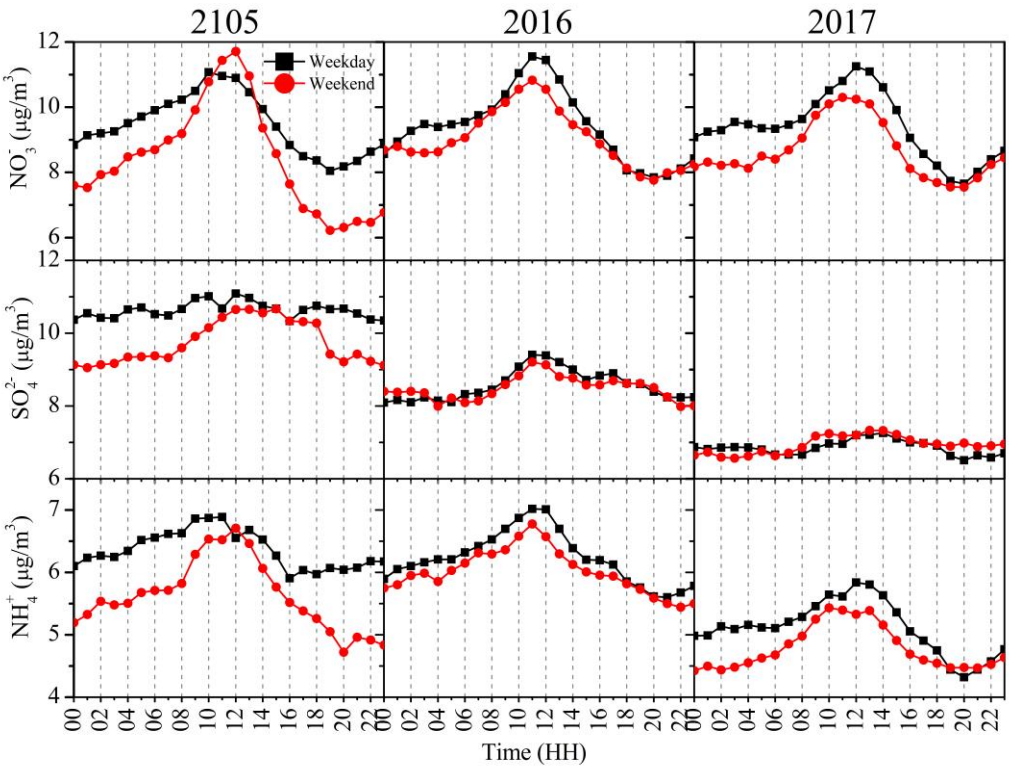

Fig. S9. Diurnal variations in NSA during weekdays and weekends from 2015 to 2017.

Table S2. Correlation analysis of Fe and Mn concentrations with SOR and NOR under different $PM_{2.5}$ concentrations.

		(Fe+Mn) under different $PM_{2.5}$ concentrations					
		0-50	50-100	100-150	150-200	200-250	>250
SOR	R^2	0.0061	0.0989	0.1118	0.0245	-0.0010	-0.0007
	r	-0.0789**	-0.3149**	-0.3352**	-0.1593**	0.0264	0.0416
	k	-0.0412	-0.0968	-0.0898	-0.0386	0.0062	0.0086
NOR	R^2	0.0014	0.0418	0.0036	0.0258	0.1132	0.1544
	r	0.0392**	-0.2050**	-0.0645**	0.1632**	0.3384**	0.3952**
	k	0.0083	-0.0285	-0.0081	0.0203	0.0408	0.0423

R^2: Coefficient of determination of the regression analysis; r: Pearson's correlation coefficient; k: Slope of regression analysis; **: Level of significance: $p < 0.01$.

ISORROPIA-II thermodynamic model sensitivity analysis

The sensitivity analysis of NSA was simulated by changing the pollutant concentration input into the ISORROPIA-II thermodynamic model by controlling the variable method. Variables: SO_4^{2-}, NO_3^- and NH_3 (measurement data during observation periods); Invariants: temperature (T), RH, Na^+, Cl^-, Ca^{2+}, K^+ and Mg^{2+} (mean values of measurement data during observation periods). For example, to study the response of ammonium and nitrate to changes in sulfate concentration, the Variable is SO_4^{2-} and Invariants include temperature (T), RH, Na^+, Cl^-, Ca^{2+}, K^+, Mg^{2+}, NO_3^- and NH_3. The degree of response is expressed by the coefficient of variation: standard deviation/mean value*100.

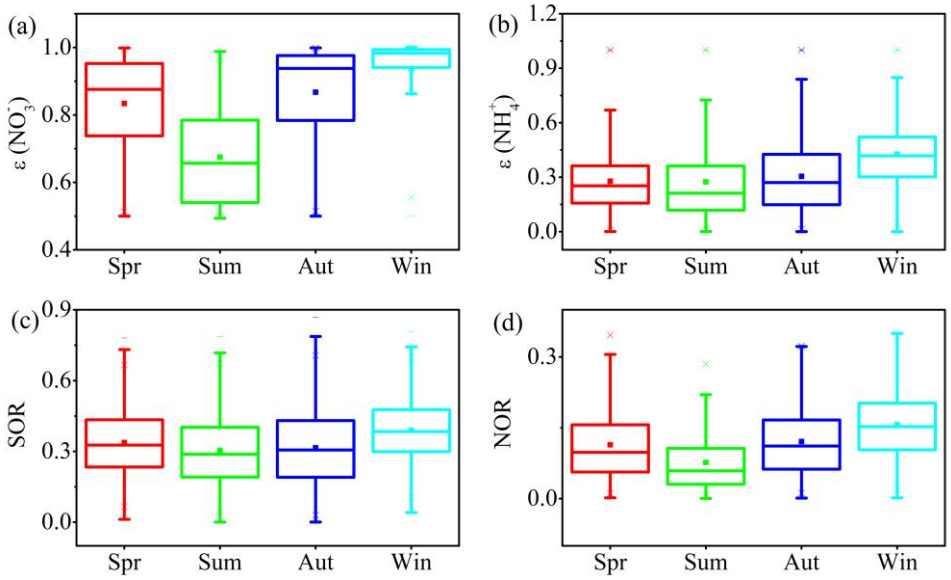

Fig. S10. (a) Gas-particle phase partitioning of NO_3^-. (b) Gas-particle phase partitioning of NH_4^+. (c) SOR. (d) NOR.

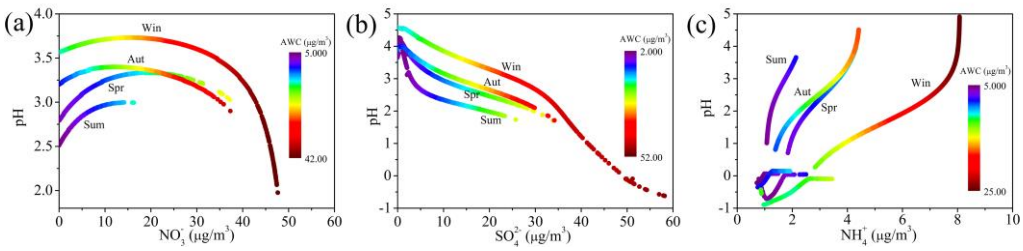

Fig. S11. The effect of changes in NO_3^-, SO_4^{2-}, NH_4^+ and aerosol water content (AWC) on pH.

Table S3. Simulation of NSA emission reduction control effect (%) and its influence on pH based on the ISORROPIA-II thermodynamic model.

Reduction	Only Reduction NO_3^-				Only Reduction SO_4^{2-}				Only Reduction NH_3				Synergistic			
	NO_3^-	SO_4^{2-}	NH_4^+	PH	NO_3^-	SO_4^{2-}	NH_4^+	PH	NO_3^-	SO_4^{2-}	NH_4^+	PH	NO_3^-	SO_4^{2-}	NH_4^+	PH
5%	14.48	5.31	18.46	3.56	9.81	9.95	18.84	3.60	11.69	5.44	17.59	3.49	15.06	10.26	21.63	3.57
10%	18.62	5.30	20.35	3.57	9.25	14.97	21.11	3.67	13.18	5.86	18.72	3.43	19.70	15.14	26.67	3.61
15%	22.81	5.29	22.26	3.63	8.77	19.99	23.35	3.73	14.93	6.33	20.01	3.37	24.37	20.04	31.65	3.63
20%	27.05	5.28	24.20	3.60	8.30	25.01	25.63	3.82	16.99	6.96	21.52	3.29	29.01	25.04	36.63	3.69

Synergistic: simultaneous emissions reductions of NO_3^-, SO_4^{2-} and NH_3

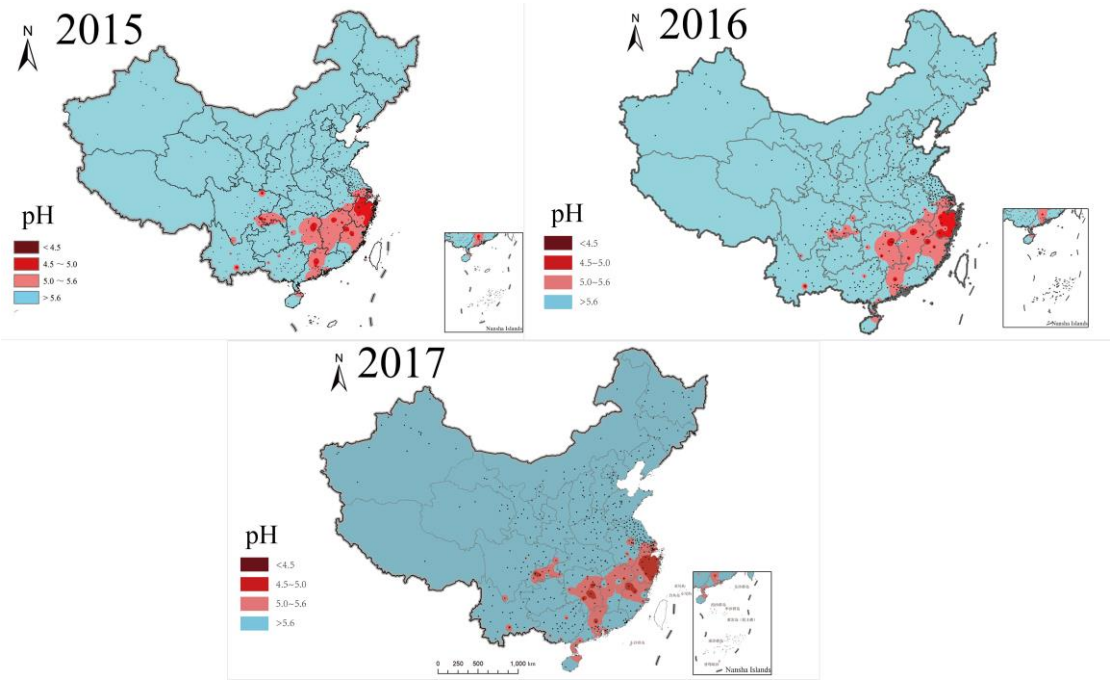

Fig. S12. Acid rain distribution in China (http://www.mee.gov.cn/hjzl/zghjzkgb/lnzghjzkgb/, last access: 12 February 2020).

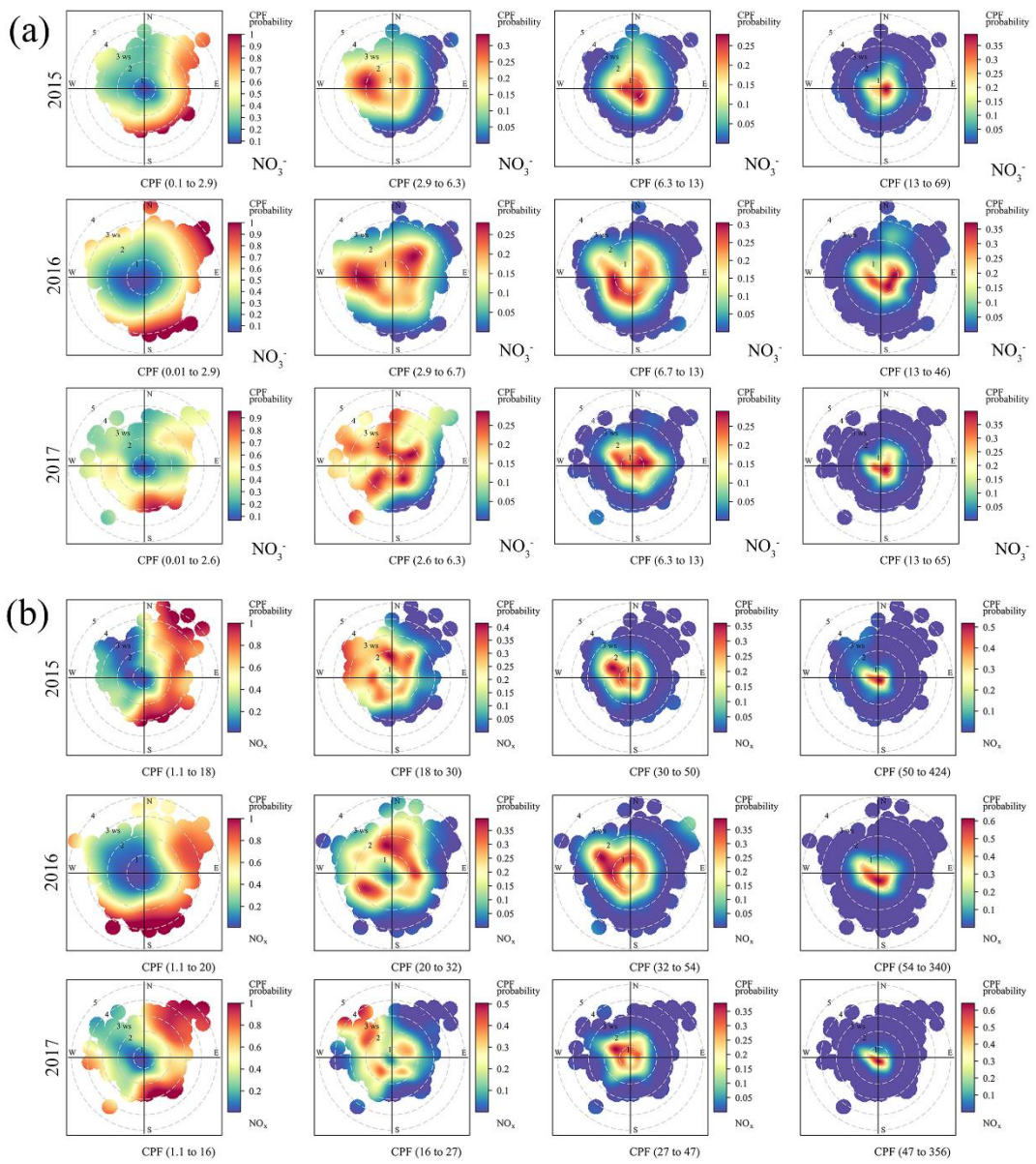

Fig. S13. PolarPlot of the NO_3^- (μg/m^3) and NOx (ppb) concentrations from 2015 to 2107 in Chengdu based on the conditional probability functions (CPF) for the following ranges of percentile intervals: 0-25%, 25-50%, 50-75%, and 75-100%. (a) NO_3^-. (b) NOx.

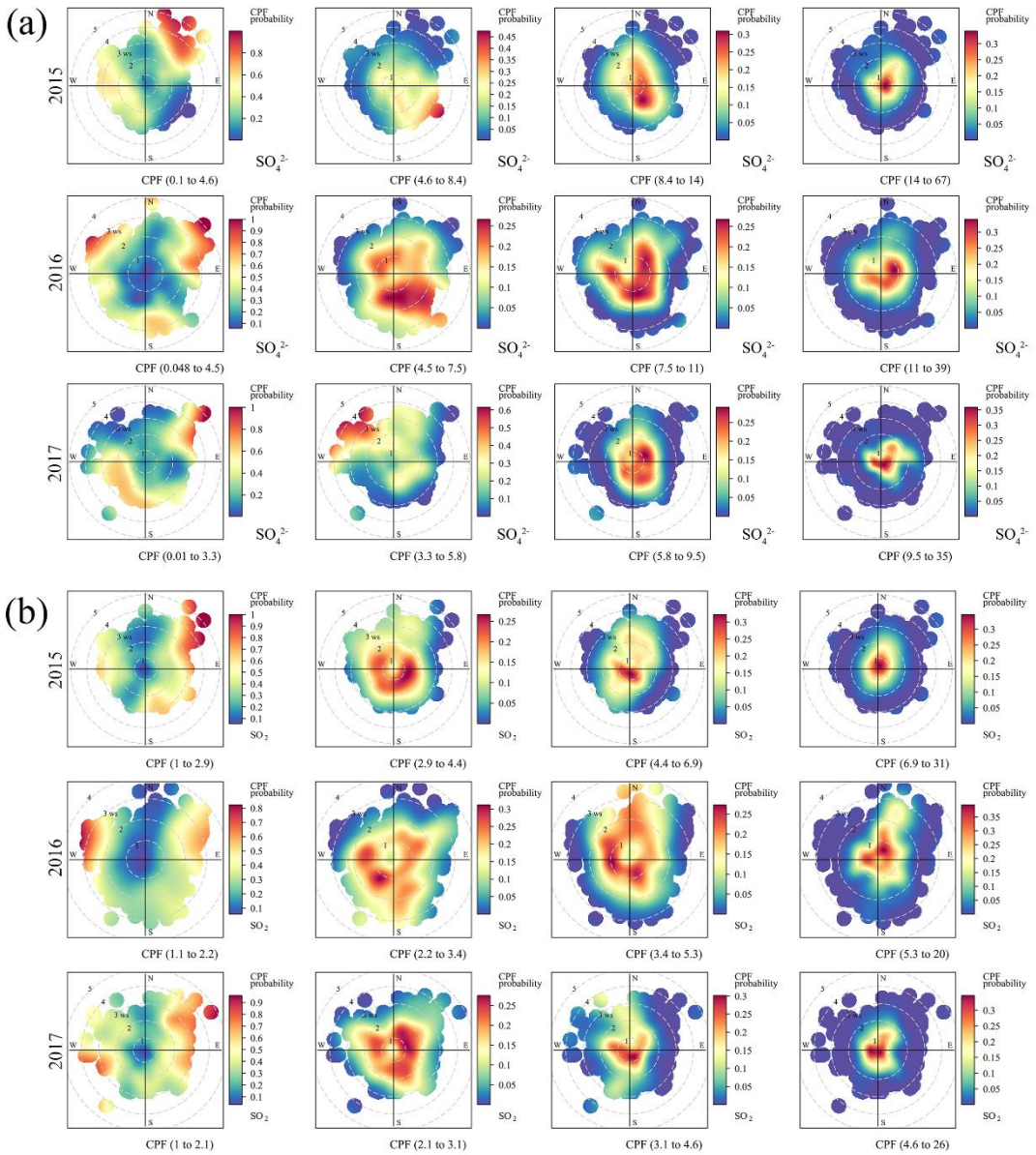

Fig. S14. PolarPlot of the SO_4^{2-} (μg/m^3) and SO_2 (ppb) concentrations from 2015 to 2107 in Chengdu based on the CPF for the following ranges of percentile intervals: 0-25%, 25-50%, 50-75%, and 75-100%. (a) SO_4^{2-}. (b) SO_2.

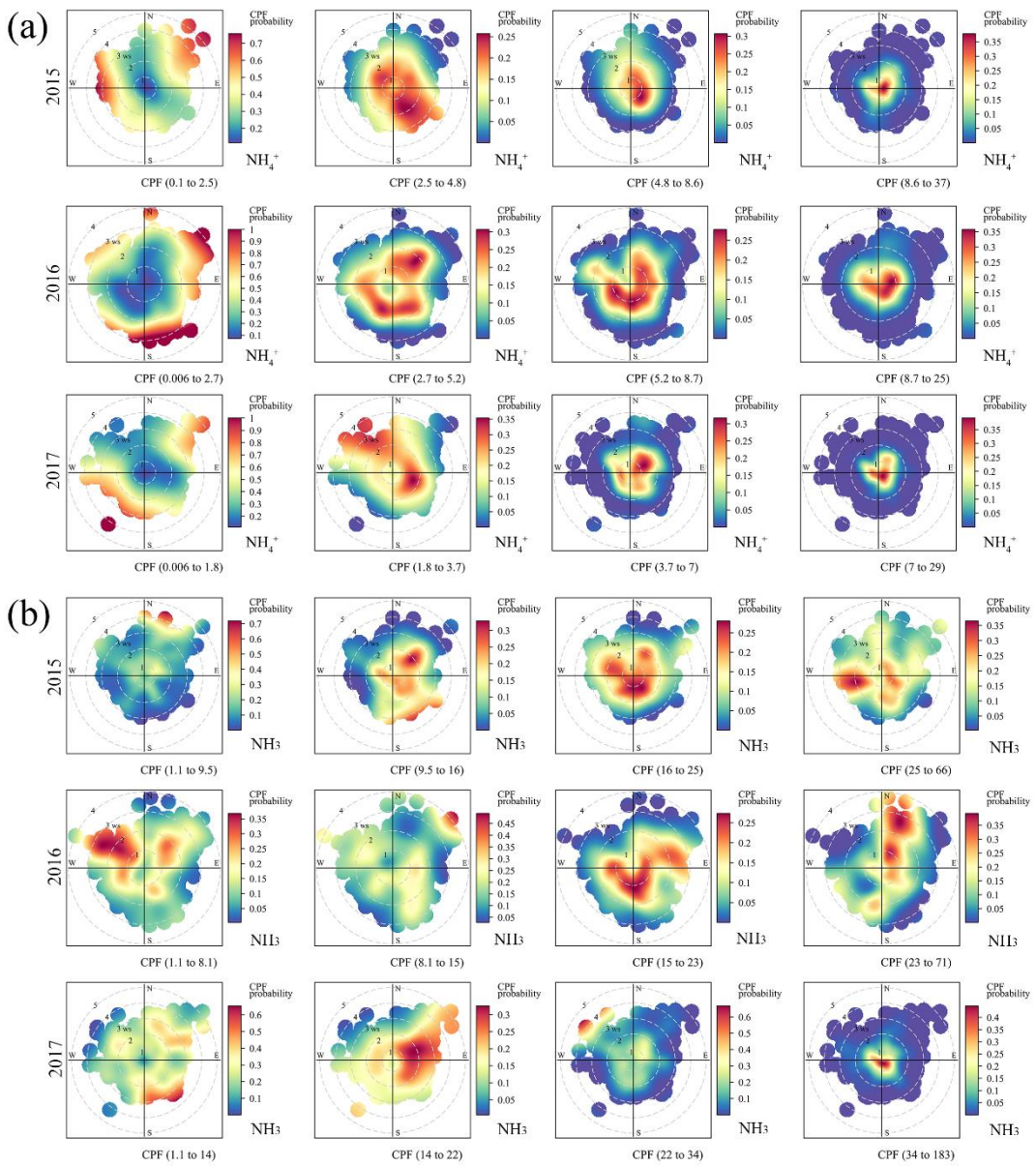

Fig. S15. PolarPlot of the NH_4^+ (μg/m^3) and NH_3 (ppb) concentrations from 2015 to 2017 in Chengdu based on the CPF for the following ranges of percentile intervals: 0-25%, 25-50%, 50-75%, and 75-100%. (a) NH_4^+. (b) NH_3.

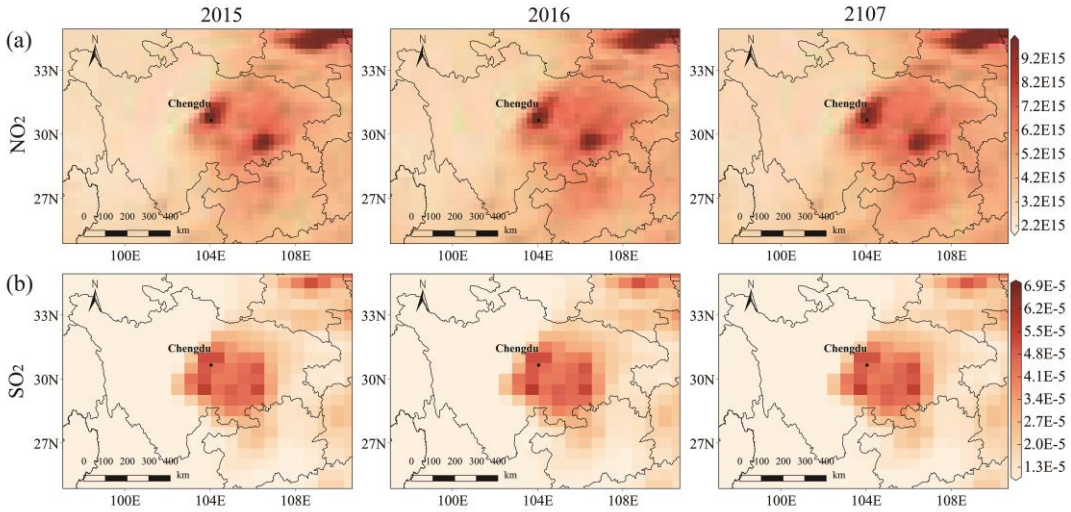

Fig. S16. Spatial distribution characteristics of NO_2 and SO_2 in the Sichuan Basin in Southwest China from 2015 to 2017. (Data are from https://giovanni.gsfc.nasa.gov/giovanni/, last access: 12 February 2020). (a) Nitrogen dioxide (NO_2) total column (30% cloud screened) ($1/cm^2$), data source: OMI. (b) Sulfur dioxide (SO_2) column mass density (kg/m^2), data source: MERRA-2 Model.

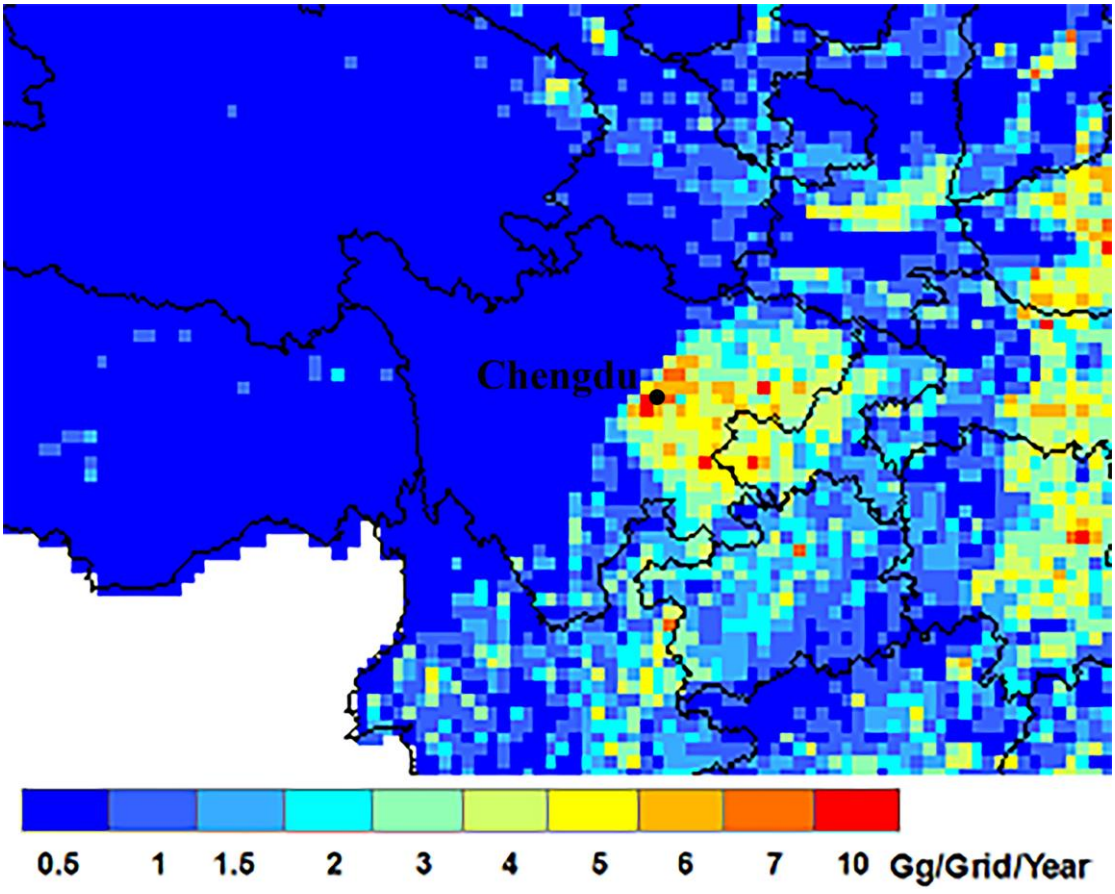

Fig. S17. Gridded NH_3 emissions in southwest China in 2016 from the Multiresolution Emission Inventory for China (MEIC, website: www.meicmodel.org, last access: 12 February 2020).